Journal of Physics B: Atomic, Molecular and Optical Physics

PAPER

Pressure shifts in high-precision hydrogen spectroscopy: II. Impact approximation and Monte-Carlo simulations

To cite this article: A Matveev *et al* 2019 *J. Phys. B: At. Mol. Opt. Phys.* **52** 075006

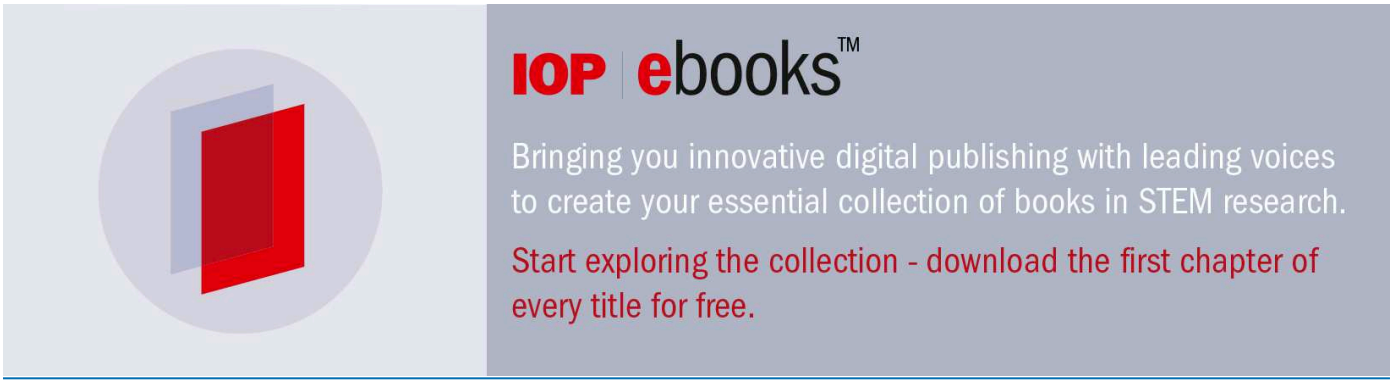

IOP Publishing Journal of Physics B: Atomic, Molecular and Optical Physics
J. Phys. B: At. Mol. Opt. Phys. **52** (2019) 075006 (15pp) https://doi.org/10.1088/1361-6455/ab08e1-1

Pressure shifts in high-precision hydrogen spectroscopy: II. Impact approximation and Monte-Carlo simulations

A Matveev[1,2], N Kolachevsky[1,3], C M Adhikari[4] and U D Jentschura[4,5]

[1] P N Lebedev Physics Institute, Leninsky prosp. 53, Moscow, 119991, Russia
[2] Max–Planck–Institut für Quantenoptik, Hans–Kopfermann-Straße 1, D-85748, Garching, Germany
[3] Russian Quantum Center, Business–Center 'Ural', 100A Novaya street, Skolkovo, Moscow, 143025, Russia
[4] Department of Physics, Missouri University of Science and Technology, Rolla, MO 65409, United States of America

E-mail: ulj@mst.edu

Received 2 November 2018, revised 11 January 2019
Accepted for publication 20 February 2019
Published 19 March 2019

Abstract

We investigate collisional shifts of spectral lines involving excited hydrogenic states, where van der Waals coefficients have recently been shown to have large numerical values when expressed in atomic units. Particular emphasis is laid on the recent hydrogen $2S$–$4P$ experiment (and an ongoing $2S$–$6P$ experiment) in Garching, but numerical input data are provided for other transitions (e.g. involving S states), as well. We show that the frequency shifts can be described, to sufficient accuracy, in the impact approximation. The pressure related effects were separated into two parts, (i) related to collisions of atoms inside of the beam, and (ii) related to collisions of the atoms in the atomic beam with the residual background gas. The latter contains both atomic as well as molecular hydrogen. The dominant effect of intra-beam collisions is evaluated by a Monte-Carlo simulation, taking the geometry of the experimental apparatus into account. While, in the Garching experiment, the collisional shift is on the order of 10 Hz, and thus negligible, it can decisively depend on the experimental conditions. We present input data which can be used in order to describe the effect for other transitions of current and planned experimental interest.

Keywords: collisional shift, collisional broadening, van der Waals interaction, impact approximation, Monte-Carlo approach

(Some figures may appear in colour only in the online journal)

1. Introduction

High-precision spectroscopy experiments on atomic hydrogen [1–5] are critically important sources of data for the least-square adjustment of fundamental constants [6]. The discrepancy in the interpretation of the results of related experiments, notably, in extracting the proton charge radius from ordinary hydrogen versus muonic hydrogen (known as the proton size puzzle, see [7, 8]), raises questions concerning conceivable systematic effects which can be overlooked in experiments. Among these, pressure-related effects (collisional shifts) need to be studied in more detail.

The absence of efficient laser-cooling techniques for atomic hydrogen makes it very difficult to devise collision-free methods of spectroscopy, e.g. those based on optical lattices. A standard method, which may be used for an immediate experimental evaluation of collisional shifts, is based on the variation of the pressure (extrapolating the spectroscopic results to vanishing particle density). However, the extrapolation procedure is also connected with an uncertainty, which affects the resulting uncertainty of the experiment. In general, if the magnitude of the pressure-related shifts in the experiment is smaller than or comparable to its overall uncertainty (due to other effects), then it is difficult to use an extrapolation procedure effectively. Under these conditions, theoretical estimates of the collisional shift become

[5] Author to whom any correspondence should be addressed.

indispensable. The simplicity of the hydrogen atom helps in this regard.

From a historical perspective, it is interesting to note that the study of collisional shifts and broadening mechanisms was started more than a century ago [9, 10]. However, the application of the developed methods to precision spectroscopy requires some efforts. The spectroscopy of atomic hydrogen takes place in atomic beams, where the distribution of relative velocities between atoms cannot be described by a simple function, like the Maxwell distribution. The geometry of the atomic beam and the velocity-selectivity of the data acquisition may also affect the evaluation. Because of the $1/R^6$ dependence of the van der Waals interaction of atoms, the effective range of the interatomic interaction is limited to a few hundred Bohr radii, and the collisions happen very fast when measured in terms of typical lifetimes of excited atomic states. This observation justifies, as we shall discuss in detail in the following, the so-called impact approximation [11] which describes the effect of the collisions as sequences of 'sudden' phase shifts, which in turn depend on the impact parameter and on the velocity of the atoms. Hence, details of the experimental apparatus need to be considered in the theoretical calculation.

The goal of this paper is to describe in detail, a procedure for the estimation of both frequency shifts as well as line broadening in precision atomic-beam measurements of transitions in hydrogen and other simple atomic systems. Particular focus will be laid on the collisional shift in the recently completed $2S$–$4P$ experiment, on a beam of cold atomic hydrogen in Garching [1]. However, we emphasize that the results of this work can also be used for future experiments on spectroscopy of other $2S$–nP transitions on the same apparatus (e.g. for $n = 6$), and with minor modifications, for other transitions which will be the focus of attention in the future. Recent progress in the determination of interaction potentials between neutral hydrogen atoms and higher excited hydrogen atoms and molecules [12–14] opens the possibility for an improved calculation of the collisional cross-sections and the corresponding shift and line broadening.

In beam spectroscopy experiments, it is convenient to separately consider the collisions of the atoms inside the beam with each other (intra-beam collisions) and collisions of the atoms with the background gas. The beam-background shift is related to the pressure of the background gas, while the intra-beam shift is related to the flux of gas. The estimation of the intra-beam shift can in principle be done analytically, and supplemented by a Monte-Carlo approach. The beam-background collisional shift can be estimated analytically, using as input the residual pressure of background gas in the vacuum chamber, which in our case is better than 10^{-8} mbar.

We organize this paper as follows: in section 2, we present a brief discussion of the basic physical ideas, and of the impact approximation used for our analysis. In section 3, we derive the cross-sections for the collisional shift in H–H collisions, using recently obtained results for the long-range van der Waals interaction coefficients. The calculation of the collisional shift for the already mentioned $2S$–$4P$ experiment and estimation of this effect for a possible upcoming $2S$–$6P$ transition measurement are completed in section 4. Conclusions are drawn in section 5. SI mksA units are used throughout the paper, in order to enhance the readability and reproducibility of the obtained results.

2. Impact approximation

A standard method to find the pressure shift in a rarified gas is based on the so-called impact approximation (see ch 36 of [15]). The main assumption of this approximation is that we can neglect the interaction of the spectator atom with the perturbing species except for a very short period of time, when perturbing atoms approach the spectator closely. For this approximation to be valid, the collision has to happen on time scales short compared to the natural lifetime of the excited atomic state. In the framework of the impact approximation, we thus neglect the duration of the collision $\tau_{\rm col}$ and consider the process as instantaneous, assuming that $\tau_{\rm col} \ll \Gamma^{-1}$, where Γ is the decay constant (imaginary part of the excited-state energy) of the atomic levels. For example, the collision time in the Garching $2S$–$4P$ experiment can be estimated in terms of the so-called Weisskopf radius, which is a critical value of an impact parameter where the phase change during a collision reaches the value of unity. (In general, a larger Weisskopf radius implies a stronger interatomic interaction.) The Weisskopf radius for the Garching $2S$–$4P$ experiment is less or on the order of $100a_0$, and the collision velocity is in the order of $300\ {\rm m\,s^{-1}}$. Thus, $\tau_{\rm col} \sim 10^{-10}$ s, while the natural lifetime of the $4P$ state is about 1.24×10^{-8} s [16], which justifies the use of the impact approximation.

Let us consider a two-level atom with an initial state $|g\rangle$ and an excited state $|e\rangle$, and an energy difference between those levels equal to $\hbar\omega_0$. The free evolution of the off-diagonal matrix element between those states can be written as $\rho_{ge}(t) = \rho_{ge}(0)\exp(-{\rm i}\,\omega_0\,t)$. The collisions with other atoms affect the phase of the oscillations, causing a drift of the phase, which we can associate with a shift and a broadening of the line via a Fourier transformation. So, we can write the oscillating term of the off-diagonal matrix element as:

$$f(t) = \exp[-{\rm i}\,\omega_0 t - {\rm i}\,\psi(t)], \tag{1}$$

where ψ is a random function, describing the total phase acquired during a collision. Within our approximations, the collision happens instantaneously, and we can write

$$\psi(t) = \sum_i \phi_i\,\Theta(t - t_i), \tag{2}$$

where Θ is the Heaviside step function, ϕ_i is a phase shift gained in ith collision, while t_i is the time of the ith event. The autocorrelation function of this oscillating process is

$$\begin{aligned} A(\tau) &= \langle f(t) f^*(t-\tau)\rangle \\ &= {\rm e}^{-{\rm i}\omega_0\tau}\langle \exp[-{\rm i}\{\psi(t) - \psi(t-\tau)\}]\rangle, \end{aligned} \tag{3}$$

where $\langle\ldots\rangle$ represents the averaging on time axis. We will assume that all collisions happen independently of each other and the distributions do not posses memory. This corresponds to a Markov process, which can be described by Poisson statistics. The probability of a collision with phase shift ϕ can be described by introducing a density function $a(\phi)$, whose

physical meaning is that

$$\mathrm{d}p = a(\phi)\,\mathrm{d}t\,\mathrm{d}\phi \tag{4}$$

is the probability of collision with a phase shift between ϕ and $\phi + \mathrm{d}\phi$ during the time interval $\mathrm{d}t$. According to the Poisson distribution, the number of the collisions k with a phase shift in the interval $(\phi,\ \phi + \mathrm{d}\phi)$ during the time τ is distributed as

$$p(k) = \frac{\lambda^k}{k!}e^{-\lambda},\ \ \lambda = a(\phi)\,\tau\,\mathrm{d}\phi. \tag{5}$$

The average value $\langle \exp(-\mathrm{i}k\phi)\rangle$ can be computed easily,

$$\begin{aligned}\langle \exp(-\mathrm{i}k\phi)\rangle &= \sum_{k=0}^{\infty} p(k)e^{-\mathrm{i}k\phi}\\ &= \sum_{k=0}^{\infty}\frac{\lambda^k e^{-\lambda-\mathrm{i}k\phi}}{k!} = \exp\left[-\lambda(1-\mathrm{e}^{-\mathrm{i}\phi})\right].\end{aligned} \tag{6}$$

In order to continue, we discretize the space of ϕ to the finite set of values $\phi_1, \phi_2, \ldots, \phi_q$, paying attention that in the end, we need to study the behavior of the equation in the limit of $q \to \infty$. It is easy to show that when we consider collisions with different values of ϕ, this formula can be generalized to the form

$$\begin{aligned}\langle \mathrm{e}^{-\mathrm{i}(\psi(t)-\psi(t-\tau))}\rangle &= \left\langle \exp\left(-\mathrm{i}\sum_{j=1}^{q}k_j\phi_j\right)\right\rangle\\ &= \left\langle \prod_{j=1}^{q}\exp(-\mathrm{i}k_j\phi_j)\right\rangle\\ &= \sum_{k_1=0}^{\infty}p(k_1)\sum_{k_2=0}^{\infty}p(k_2)\cdots\sum_{k_j=0}^{\infty}p(k_j)\cdots\\ &\quad \sum_{k_q=0}^{\infty}p(k_q)\prod_{j=1}^{q}\exp(-\mathrm{i}k_j\phi_j)\\ &= \prod_{j=1}^{q}\sum_{k_j=0}^{\infty}p(k_j)\exp(-\mathrm{i}k_j\phi_j)\\ &= \prod_{j=1}^{q}\exp(-\lambda_j)\sum_{k_j=0}^{\infty}\frac{\lambda_j^{k_j}}{k_j!}\exp(-\mathrm{i}k_j\phi_j).\end{aligned} \tag{7}$$

With the help of equation (6), we may express this as

$$\begin{aligned}\langle \mathrm{e}^{-\mathrm{i}(\psi(t)-\psi(t-\tau))}\rangle &= \prod_{j=1}^{q}\langle\exp(-\mathrm{i}k_j\phi_j)\rangle\\ &= \prod_{j=1}^{q}\exp\left[-\lambda_j(1-\exp(-\mathrm{i}\phi_j))\right]\\ &= \exp\left(-\sum_{j=1}^{q}\lambda_j(1-\exp(-\mathrm{i}\phi_j))\right).\end{aligned} \tag{8}$$

In the limit of q approaching infinity, one can express the sum on the right-hand side of equation (8), in integral form, as

$$\begin{aligned}&\langle e^{-\mathrm{i}(\psi(t)-\psi(t-\tau))}\rangle\\ &= \exp\left(-\tau\int_{-\infty}^{\infty}a(\phi)\left[1-\mathrm{e}^{-\mathrm{i}\,\phi}\right]\mathrm{d}\phi\right)\\ &= \exp\left(-\tau\int_{-\infty}^{\infty}a(\phi)[1-\cos\phi]\,\mathrm{d}\phi\right)\\ &\quad\times\exp\left(-\mathrm{i}\,\tau\int_{-\infty}^{\infty}a(\phi)\sin\phi\,\mathrm{d}\phi\right),\end{aligned} \tag{9}$$

where we make use of $\lambda = a(\phi)\,\tau\,\mathrm{d}\phi$. The phase factor has to be added to the phase $\exp(-\mathrm{i}\omega_0 t)$ from equation (3). According to the Wiener–Khinchin theorem, the power spectrum of the process $f(t)$ can be obtained by Fourier transform of the auto-correlation function. This calculation gives a Lorentz function

$$\tilde{f}(\omega) \sim \frac{(\gamma_c/2)^2}{(\gamma_c/2)^2 + (\omega-\omega_0-\omega_c)^2}, \tag{10}$$

where ω_c and γ_c are obtained as the collisional shift and broadening:

$$\omega_c = \int_{-\infty}^{+\infty}a(\phi)\sin(\phi)\,\mathrm{d}\phi, \tag{11}$$

$$\gamma_c = \int_{-\infty}^{+\infty}a(\phi)\,[1-\cos(\phi)]\,\mathrm{d}\phi. \tag{12}$$

The physical dimension of these equations can easily be checked upon observing that $a(\phi)$, according to equation (4), carries a physical dimension of inverse time.

3. Calculation of collisional shifts and broadenings

3.1. Peculiarities of van der Waals coefficients for S states

Even if the main subject of the current paper is the pressure shift in $1S$–nP transition, we here recall a few interesting aspects of calculations related to van der Waals interactions of atomic hydrogen atoms in S states. We consider a two-atom system in which both atoms A and B are in $|kS\rangle$ and $|nS\rangle$, where $k, n \in \mathbb{N}$. The energetic degeneracy of states $|kS\rangle_A|nS\rangle_B$ and $|nS\rangle_A|kS\rangle_B$ indicates that the kS–nS exchange interaction results in entanglement of the states, whose basis states are

$$|\Psi_1\rangle = |kS\rangle_A|nS\rangle_B \text{ and } |\Psi_2\rangle = |nS\rangle_A|kS\rangle_B. \tag{13}$$

The eigenvalue equation of the system is given by

$$(H_0 + H_{\mathrm{vdW}})|\Psi\rangle = E|\Psi\rangle, \tag{14}$$

where the unperturbed Hamiltonian H_0 is the sum of the Schrödinger Hamiltonians of the atoms,

$$H_0 = \sum_{i=A,B}\left(\frac{\vec{p}_i^{\,2}}{2m} - \frac{e^2}{4\pi\epsilon_0}\frac{1}{|\vec{r}_i|}\right). \tag{15}$$

Here, m is the mass of the electron, while $\vec{p}_i$ and $\vec{r}_i$ are the kinetic momenta of the electron for an atom i and the position of the electron relative to the nucleus of the atom, respectively. The van der Waals Hamiltonian,

$$H_{\mathrm{vdW}} = \frac{e^2}{4\pi\epsilon_0}\frac{x_A\,x_B + y_A\,y_B - 2\,z_A\,z_B}{R^3}, \tag{16}$$

is the perturbation to the system. Here x_i, y_i, and z_i are the coordinates of the atomic electrons with respect to the atomic centers, while R is the interatomic distance. As given in section 4 of [12], the eigenenergies and the eigenvectors of the system, in the van der Waals range ($a_0 \ll R \ll a_0/\alpha$),

can be expressed as

$$E_{\pm} = E_0 - \frac{D_6(nS;\, kS) \pm M_6(nS;\, kS)}{R^6}, \tag{17a}$$

$$|\Psi\rangle = \frac{1}{\sqrt{2}}(|\Psi_1\rangle \pm |\Psi_2\rangle), \tag{17b}$$

where E_0 is the unperturbed energy, and $D_6(nS;\, kS)$ and $M_6(nS;\, kS)$ are, respectively, the direct and mixing van der Waals coefficients. They are given by equation (54) of [12]. Let us recall them here for convenience,

$$D_6(nS;\, kS) = \frac{2\, e^4}{3(4\pi\epsilon_0)^2} \times \sum\!\!\!\!\!\!\int_{pq} \frac{|\langle kS|\vec{r}\ |p\rangle|^2 |\langle nS|\vec{r}\ |q\rangle|^2}{E_p + E_q - (E_{kS} + E_{nS})}, \tag{18a}$$

$$M_6(nS;\, kS) = \frac{2\, e^4}{3(4\pi\epsilon_0)^2} \times \sum\!\!\!\!\!\!\int_{pq} \frac{\langle kS|\vec{r}\ |p\rangle \cdot \langle p|\vec{r}|nS\rangle \langle nS|\vec{r}\ |q\rangle \cdot \langle q|\vec{r}\ |kS\rangle}{E_p + E_q - (E_{kS} + E_{nS})}. \tag{18b}$$

Here, the sum-integral sign clarifies that the continuum states are to be included in the sum over virtual states, and the transition matrix elements are to be evaluated for the two atoms separately, as indicated. The symmetry-dependent quantity $D_6(nS;\, kS) \pm M_6\ (nS;\, kS)$ is the van der Waals coefficient of the nS–kS system. More explicitly,

$$C_6(nS;\, kS) = D_6(nS;\, kS) \pm M_6(nS;\, kS). \tag{19}$$

For example, the coefficients $C_6(2S;\, 1S)$ (see [12]) and $C_6(3S;\, 1S)$ (see [17]) are given as

$$C_6(2S;\, 1S) = (176.752\,266 \pm 27.983\,245)\, E_h\, a_0^6, \tag{20a}$$

$$C_6(3S;\, 1S) = (917.478\,571 \pm 2.998\,270)\, E_h\, a_0^6, \tag{20b}$$

where $E_h = \alpha^2 mc^2$ and $a_0 = \hbar/(\alpha mc)$ are the Hartree energy and the Bohr radius, respectively. (In atomic units, both E_h and a_0 are unity.) Notice that, for the $2S$–$1S$ system, the D_6 coefficient is about six times larger than the M_6 coefficient whereas for the $3S$–$1S$ system the D_6 coefficient is two orders of magnitude larger than the M_6 coefficient. The M_6 coefficient becomes smaller with the principal quantum number is being increased as recently observed in [17]. However, the D_6 coefficients increase as the fourth power of the principal quantum number of the excited reference states. As a consequence, the mixing M_6 coefficient becomes negligible in comparison to the direct D_6 coefficient for higher excited reference states.

3.2. Peculiarities of van der Waals coefficients for P states

For interactions involving higher excited P states (in atomic hydrogen), other issues arise. Namely, in a sum-over-states representation (see equation (18*a*) and appendix A), the van der Waals C_6 coefficient is obtained in terms of dipole transitions of the two atoms to virtual levels accessible via such transitions, with the sum of the transition frequencies for the virtual transitions of both atoms in the denominator. The C_6 coefficients in the nP–$1S$ and nP–$2S$ systems are enhanced because of the presence of quasi-degenerate virtual states which are accessible via such transitions. This is illustrated in figure 1 for the $4P$–$1S$ system: An allowed one-photon exchange from an initial $(1S;\, 4P)$ state couples to the quasi-degenerate $(4P;\, 1S)$ level. Therefore, hyperfine frequencies enter the propagator denominator in second-order perturbation theory, and the C_6 coefficient is drastically enhanced [14].

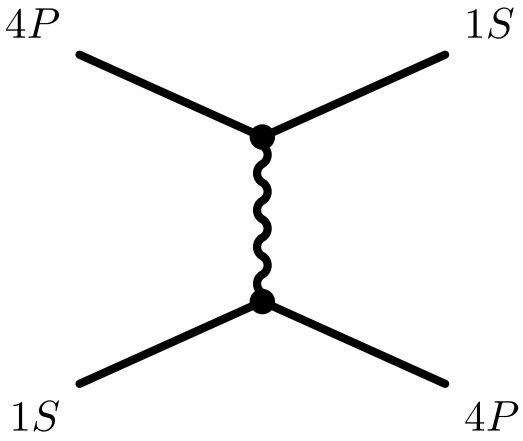

Figure 1. One-photon exchange from a $(4P;\, 1S)$ atomic hydrogen state to a $(1S;\, 4P)$ state, for long-range interactions between two atoms.

For example, we have according to equation (69) of [14] for the $4P$–$1S$ system,

$$\langle C_6(4P_{1/2};\, 1S)\rangle = 2.489 \times 10^4\, E_h\, a_0^6, \tag{21a}$$

$$\langle C_6(4P_{3/2};\, 1S)\rangle = -1.245 \times 10^4\, E_h\, a_0^6. \tag{21b}$$

Here, by $\langle C_6\rangle$, we denote a linear average over the hyperfine manifolds has been performed, which is (slightly) different over the averaging procedure required for the calculation of the pressure shift (see appendix B). Specifically, one has $\langle |C_6|^{2/5}\rangle \neq |\langle C_6\rangle|^{2/5}$. (Numerical experiments show that the two quantities differ by no more than 30% for typical atomic transitions in hydrogen.) By contrast, for the $6P$–$1S$ system, we have according to equation (27) of [18],

$$\langle C_6(6P_{1/2};\, 1S)\rangle = -8.234\,7 \times 10^2\, E_h\, a_0^6, \tag{22a}$$

$$\langle C_6(6P_{3/2};\, 1S)\rangle = 4.117\,4 \times 10^2\, E_h\, a_0^6, \tag{22b}$$

so the sign pattern is reversed as compared to the $4P$–$1S$ system.

The enhancement of C_6 could of course only occur if the two atomic or molecular species involved in the long-range interaction have identical or very similar transition frequencies. Typically, this would be the case for identical atoms or molecules, or closely related ones, like different isotopes. For the reference $(4P;\, 1S)$ system, the virtual transition frequency to $(1S;\, 4P)$ is almost zero because the two virtual transition frequencies for the two atoms (almost) cancel. The first-order perturbation, for absolute degeneracy, is treated in appendix A.

3.3. Cross sections

In order to establish a connection between the gas model and the oscillator model, we can parameterize all collisions by the relative velocity of the colliding atoms v and the impact parameter b. If we write the interaction between the spectator atom in the state $|s\rangle$ ($s = g, e$) and the perturbing atom at a distance R as $E_s(R)$, then the phase shift in a single collision can be calculated in non-recoil limit as

$$\phi(v, b) = \frac{1}{\hbar}\int_{-\infty}^{+\infty}(E_e(\sqrt{v^2t^2 + b^2}) - E_g(\sqrt{v^2t^2 + b^2}))\mathrm{d}t. \tag{23}$$

In order to convert the formulas (11) and (12) into cross sections, we should recall that $\mathrm{d}p/\mathrm{d}t = a(\phi)\,\mathrm{d}\phi$, and that

$$\left(\frac{\mathrm{d}A\ \mathrm{d}p}{\mathrm{d}N}\right) = 2\pi b\ \mathrm{d}b = \left(\frac{\mathrm{d}t\ \mathrm{d}A}{\mathrm{d}N}\right)\left(\frac{\mathrm{d}p}{\mathrm{d}t}\right) = \left(\frac{1}{\mathfrak{n}v_c}\right)(a(\phi)\ \mathrm{d}\phi), \tag{24}$$

where $\mathrm{d}N$ is an infinitesimal number of atoms, $\mathrm{d}A$ is a cross-sectional impact area, and $\mathfrak{n}$ is the number density of the atoms. Also, v_c is the velocity of collisions. This implies that $a(\phi)\,\mathrm{d}\phi = \mathfrak{n}v_c\ 2\pi b\ \mathrm{d}b$, where v_c is the velocity of collisions. Hence, we can compute the cross-sections of the pressure shift and broadening (in units of rad m^2):

$$\sigma_\omega(v) = \int_0^\infty 2\pi b \sin(\phi(v, b))\ \mathrm{d}b, \tag{25a}$$

$$\sigma_\gamma(v) = \int_0^\infty 2\pi b\,[1 - \cos(\phi(v, b))]\mathrm{d}b. \tag{25b}$$

With the help of the formulas for the cross-sections, we estimate the shift and broadening of the spectral line by simple formulas

$$\omega_c = \mathfrak{n}\ v_c\ \sigma_\omega(v_c), \tag{26a}$$

$$\gamma_c = \mathfrak{n}\ v_c\ \sigma_\gamma(v_c), \tag{26b}$$

where v_c is a characteristic velocity of the collisions, which will be specified in greater detail in the following. An improvement of this estimate requires a more careful consideration of the distribution of collisional velocities (e.g. with the help of a Monte Carlo simulation).

We shall also notice that in some cases the integrals in previous equations can be computed analytically. Particularly, if the interaction energy can be expressed as $E(R) = -C_nR^{-n}$, where $n = 4, 5, 6, \ldots$ is a positive integer number, then the cross-section corresponding to the pressure shift reads, in view of equation (23),

$$\sigma_\omega(v, n) = \int_0^\infty 2\pi b \sin\left(-\frac{C_n}{\hbar}\int_{-\infty}^{+\infty}(b^2 + t^2v^2)^{-n/2}\mathrm{d}t\right)\mathrm{d}b = -\mathrm{sgn}(C_n)\int_0^\infty 2\pi b \sin\left(\frac{|C_n|}{\hbar v}\sqrt{\pi}\ b^{1-n}\frac{\Gamma\left(\frac{n-1}{2}\right)}{\Gamma\left(\frac{n}{2}\right)}\right)\mathrm{d}b. \tag{27}$$

Table 1. Coefficients $A_\omega(n)$ and $A_\gamma(n)$ for $n = 4, 5, 6$.

n	$A_\omega(n)$	$A_\gamma(n)$
4	9.848 95	5.686 29
5	4.546 52	4.546 52
6	2.936 24	4.041 39

For a positive integer n, equation (27) can be expressed as

$$\sigma_\omega(v, n) = -A_\omega(n)\,\mathrm{sgn}(C_n)\left(\frac{|C_n|}{\hbar v}\right)^{2/(n-1)}, \tag{28}$$

where sgn(x) is the sign function, i.e. sgn(x) = 1 if $x > 0$ and sgn(x) = −1 if $x < 0$. Since the cross-section is just a proportionality coefficient between the flux of atoms and the experienced frequency shift, the sign of σ_ω deserves a remarks According to equation (17*a*), a positive C_6 coefficient is associated with an attractive van der Waals interaction, which in turn leads to a negative frequency shift in equation (28). In contrast to σ_ω (v, n), we shall define, in the following, the cross section σ_γ (v, n) associated with collisional broadening, as a manifestly positive quantity.

The coefficients $A_\omega(n)$ are n-dependent dimensionless constants. For $n \geqslant 4$, $A_\omega(n)$ is given by

$$A_\omega(n) = \pi^{n/(n-1)}\,\Gamma\left(\frac{n-3}{n-1}\right)\left(\frac{\Gamma\left(\frac{n-1}{2}\right)}{\Gamma\left(\frac{n}{2}\right)}\right)^{2/(n-1)} \times \sin\left(\frac{\pi}{n-1}\right). \tag{29}$$

Similarly, the cross-section corresponding to the pressure broadening for any $n \geqslant 3$ reads

$$\sigma_\gamma(v, n) = \int_0^\infty 2\pi b\left[1 - \cos\left(\frac{C_n}{\hbar v}\sqrt{\pi}\ b^{1-n}\frac{\Gamma\left(\frac{n-1}{2}\right)}{\Gamma\left(\frac{n}{2}\right)}\right)\right]\mathrm{d}b = A_\gamma(n)\left(\frac{|C_n|}{\hbar v}\right)^{2/(n-1)}. \tag{30}$$

Both the $A_\omega(n)$ and the $A_\gamma(n)$ coefficients are dimensionless. For $n > 3$, we have

$$A_\gamma(n) = \pi^{n/(n-1)}\,\Gamma\left(\frac{n-3}{n-1}\right) \times \left(\frac{\Gamma\left(\frac{n-1}{2}\right)}{\Gamma\left(\frac{n}{2}\right)}\right)^{2/(n-1)}\cos\left(\frac{\pi}{n-1}\right), \tag{31}$$

while for $n = 3$, the coefficient $A_\gamma(n = 3) = \pi^2$, and the integral for $A_\omega(n = 3)$ does not converge. We refer to table 1 for the values of $A(n)$ coefficients, for the cases $n = 4, 5, 6$.

In case of collisions between hydrogen atoms, when the interaction potential is caused by van der Waals forces, the most relevant distance region is ($a_0 \ll R \ll a_0/\alpha$). In the van der Waals region, the dipole interaction of an excited

Table 2. Coefficients of collisional broadening and frequency shift are given for hydrogen transitions of experimental interest for high-precision spectroscopy. The corresponding cross-sections can be calculated using the given data, via formula (32). The colliding system is described in the column 'perturber-spectator' in the format 'state of perturber atom–(lower state of spectator atom−upper state of spectator atom)'. The $1S$ hydrogen atoms may be present in all possible hyperfine substates, while the $2S$ atoms, in accordance with the experimental apparatus, are assumed to be in an $F = 0$ substate only, after having been excited via two-photon absorption from the $F = 0$ hyperfine ground-state sublevel. This is at variance with equations (21*a*)–(22*b*). The coefficients $\xi^{(6)}_{\omega,\gamma}$ for perturber $1S$ atoms were averaged over the manifold of all available hyperfine substates, while the $2S$ perturber atoms were taken only in the $F = 0$ substates. The averaging is done according to equation (40).

Perturber-spectator	$\xi^{(6)}_{\omega}$ (rad m^2 (m s^{-1})$^{2/5}$)	$\xi^{(6)}_{\gamma}$ (rad m^2 (m s^{-1})$^{2/5}$)
$1S$–($1S$–$2S$)	-2.232×10^{-17}	3.072×10^{-17}
$1S$–($1S$–$3S$)	-4.325×10^{-17}	5.953×10^{-17}
$1S$–($1S$–$4S$)	-6.855×10^{-17}	9.435×10^{-17}
$1S$–($2S$–$4P_{1/2}$)	3.133×10^{-16}	4.313×10^{-16}
$1S$–($2S$–$4P_{3/2}$)	-5.753×10^{-16}	7.919×10^{-16}
$1S$–($2S$–$6P_{1/2}$)	1.506×10^{-16}	2.072×10^{-16}
$1S$–($2S$–$6P_{3/2}$)	-3.172×10^{-16}	4.365×10^{-16}
$2S(F = 0)$–($1S$–$2S$)	-1.474×10^{-15}	2.029×10^{-15}
$2S(F = 0)$–($2S$–$4P_{1/2}$)	2.719×10^{-14}	3.742×10^{-14}
$2S(F = 0)$–($2S$–$4P_{3/2}$)	-1.812×10^{-14}	2.494×10^{-14}
$2S(F = 0)$–($2S$–$6P_{1/2}$)	5.053×10^{-15}	1.304×10^{-14}
$2S(F = 0)$–($2S$–$6P_{3/2}$)	-4.355×10^{-14}	5.967×10^{-14}

atom interacting with the induced dipole of the ground state atom produces van der Waals type of pressure shift and broadening. The corresponding cross-sections, for $n = 6$, are given by

$$\sigma^{(6)}_{\omega}(v) = \xi^{(6)}_{\omega} v^{-2/5}, \quad \sigma^{(6)}_{\gamma}(v) = \xi^{(6)}_{\gamma} v^{-2/5}, \tag{32}$$

where the superscript in C_6 indicates that the interactions are of the nonretarded van der Waals type and the proportionality coefficients $\xi^{(6)}_{\omega,\gamma}$ are given by

$$\xi^{(6)}_{\omega} = -\frac{3^{2/5}\sqrt{5-\sqrt{5}}}{2^{27/10}}\,\pi^{9/10}\,\Gamma\left(\frac{3}{5}\right)\mathrm{sgn}(C_6)\left(\frac{|C_6|}{\hbar}\right)^{2/5} = -2.936\,24\,\mathrm{sgn}(C_6)\left(\frac{|C_6|}{\hbar}\right)^{2/5}, \tag{33a}$$

$$\xi^{(6)}_{\gamma} = -\frac{3^{2/5}(\sqrt{5}+1)}{2^{11/5}\times 5}\,\pi^{7/5}\Gamma\left(-\frac{2}{5}\right)\left(\frac{|C_6|}{\hbar}\right)^{2/5} = 4.041\,39\left(\frac{|C_6|}{\hbar}\right)^{2/5}. \tag{33b}$$

The coefficients $\xi^{(6)}_{\omega,\gamma}$, computed for the different transitions are given in table 2. Numerically, the magnitude of the pressure-shift cross-section is about three-quarters of the pressure-broadening cross-section, as is evident from equations (33*a*) and (33*b*).

We refer to [12–14, 17, 18] for numerical values of the van der Waals C_6 coefficients. As is evident from the discussion in section 3.1, the van der Waals C_6 coefficients are symmetry dependent for nS–$1S$ interactions (see [12, 17, 19]). With D_6 denoting the 'direct' term and M_6 the 'mixing' term, one obtains the coefficients $D_6 \pm M_6$ for the symmetric and anti-symmetric combinations of the two-atom states. The coefficients $D_6 \pm M_6$ should then be taken to the power of $2/5$. Assuming an equal likelihood for collisions to take place in either of the two symmetries, appropriate formulas to evaluate the $\xi^{(6)}_{\omega}$ and $\xi^{(6)}_{\gamma}$ are given as

$$\xi^{(6)}_{\omega} = -1.468\,12\left\{\left[\mathrm{sgn}(D_6+M_6)\left(\frac{|D_6+M_6|}{\hbar}\right)^{2/5} + \mathrm{sgn}(D_6-M_6)\left(\frac{|D_6-M_6|}{\hbar}\right)^{2/5}\right] \pm \left[\mathrm{sgn}(D_6+M_6)\left(\frac{|D_6+M_6|}{\hbar}\right)^{2/5} - \mathrm{sgn}(D_6-M_6)\left(\frac{|D_6-M_6|}{\hbar}\right)^{2/5}\right]\right\}, \tag{34a}$$

$$\xi^{(6)}_{\gamma} = 2.020\,70\left\{\left[\left(\frac{|D_6+M_6|}{\hbar}\right)^{2/5} + \left(\frac{|D_6-M_6|}{\hbar}\right)^{2/5}\right] \pm \left[\left(\frac{|D_6+M_6|}{\hbar}\right)^{2/5} - \left(\frac{|D_6-M_6|}{\hbar}\right)^{2/5}\right]\right\}. \tag{34b}$$

For all nS–$1S$ systems with $n \geqslant 4$, the mixing van der Waals coefficient M_6 is smaller by at least four order of magnitude than the direct term D_6 [17]. This fact simplifies the situation. If we include the mixing term, then, for the $2S$–$1S$ system, $\xi^{(6)}_{\omega}(v)$ and $\xi^{(6)}_{\gamma}(v)$ should read as

$$\xi^{(6)}_{\omega}(2S;\,1S) = -(2.232 \pm 0.142) \times 10^{-17}\,\mathrm{rad\ m^2(m\,s^{-1})^{2/5}}, \tag{35}$$

and

$$\xi^{(6)}_{\gamma}(2S;\,1S) = (3.072 \pm 0.196) \times 10^{-17}\,\mathrm{rad\ m^2(m\,s^{-1})^{2/5}}, \tag{36}$$

respectively. The mixing term is not indicated in table 2, but given in explicit form in equations (35) and (36). For the

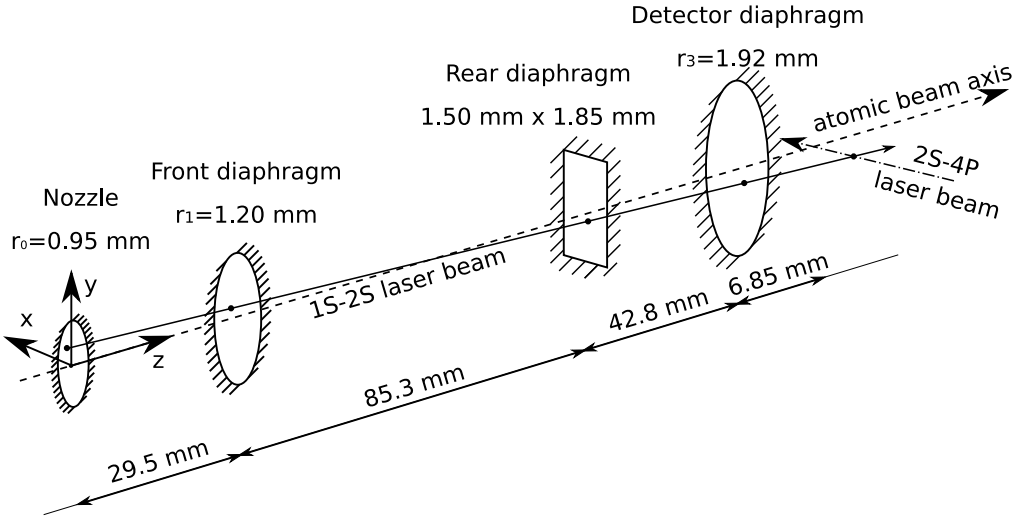

Figure 2. The scheme used for simulation of the collisional shift from intra-beam collisions. The trajectories of atoms are starting on the nozzle outlet; the diaphragms are forming the atomic beam. Atoms can be excited in $2S$ state in the $1S$–$2S$ Gaussian laser beam with $1/e^2$ intensity radius 0.3 mm. Excited $2S$ atoms crosses the $2S$–$4P$ spectroscopy laser beam. During that the $2S$–$4P$ beam the atoms can collide with other atoms from the beam, which causes an intra-beam shift. The Monte-Carlo procedure of calculation of this shift is based on random seeding of the trajectory of the spectator atom A, the trajectory of the perturber atom B in a way that they collide in point $\vec{r}_{\rm col}$, averaging a function Ω_{sv}, describing the collisional shift for different velocity groups with proper weights.

$3S$–$1S$ system, one has

$$\xi_\omega^{(6)}(3S;\,1S) = -(4.3253 \pm 0.0056) \times 10^{-17}\ \text{rad m}^2(\text{m s}^{-1})^{2/5}, \tag{37}$$

and

$$\xi_\gamma^{(6)}(3S;\,1S) = (5.9534 \pm 0.0078) \times 10^{-17}\ \text{rad m}^2(\text{m s}^{-1})^{2/5}. \tag{38}$$

The mixing contribution only enters at the third decimal. The long-range interaction potential is attractive, which means that the frequency shift is negative. Presenting our results only to four significant figures, we can neglect mixing contributions for the $4S$–$1S$ system and higher excited reference states.

In table 2, we present the average values of $\xi_\gamma^{(6)}$ and $\xi_\omega^{(6)}$ for $F = 0$ to $F = 1$ transitions in the hyperfine manifolds of the $2S$–$2S$ and $2S$–nP_J systems. Note that both $\xi_\gamma^{(6)}$ and $\xi_\omega^{(6)}$ are proportional to $|C_6|^{2/5}$. The averaging over the fine and hyperfine levels is done as follows. Let us assume that the system we are interested in has N hyperfine manifolds which we label by a subscript $j = 1, \ldots, N$, with multiplicities $\mathfrak{m}_j$, and also let $\mathbb{M} = \sum_j \mathfrak{m}_j$. The $\xi_\gamma^{(6)}$ and $\xi_\omega^{(6)}$ are calculated using

$$\xi_\omega^{(6)} = -2.936\ 24\ \text{sgn}(C_6)\ \langle |C_6|^{2/5}\rangle \big/ \hbar^{2/5}, \tag{39a}$$

$$\xi_\gamma^{(6)} = 4.041\ 39\ \langle |C_6|^{2/5}\rangle \big/ \hbar^{2/5}, \tag{39b}$$

where

$$\langle |C_6^{2/5}|\rangle = \frac{1}{\mathbb{M}} \sum_j \mathfrak{m}_j (|C_6^{(j)}|)^{2/5}. \tag{40}$$

We shall notice that in our theoretical works ([14, 18]), the energy shift for both the $1S$ and $2S$ collisions are averaged over all possible hyperfine states. The particular interest of the current work is concentrated on the $2S$–$4P$ and $2S$–$6P$ experiments at the Max Planck Institute at Garching, where atoms are prepared in the metastable $2S(F = 0)$ state [1]. Selection rules of spectroscopy allow the excitation from the $2S(F = 0)$ state to the $nP_j(F = 1)$ states, where $j = 1/2, 3/2$. So, the averaging in this case should be done over a different manifold of quantum states. We here use the van der Waals coefficients $C_6(2S(F = 0)$–$nP_j(F = 1))$ whose evaluation is described in detail in the accompanying article [14].

One may notice that in nS–mP collisions, the van der Waals Hamiltonian (16) mixes the quantum states of the system $|nS_A, mP_B\rangle$ with a state $|mP_A, nS_B\rangle$. In principle, this mixing may cause a first-order energy shift, proportional to R^{-3}. However, this first-order shift averages out to zero when taken over state manifolds; hence it does not contribute to the pressure shift [20]. Indeed, we may cite the following remark on p 1045 of [20]: 'Shifts would be given by the imaginary part of the S matrix element, but are zero for resonance dipole–dipole interactions'. Note that in the notation of [20], the S matrix element is given by the expression $\langle l|\Phi|l\rangle$. In our notation, in appendix A, the S matrix element is denoted as $\langle l|\theta|l\rangle$ in order to ensure the self-consistency of the notation we are using in this paper (more details are provided in appendix A).

4. Collisional shift in the Garching $2S$–$4P$ hydrogen experiment

4.1. Experimental apparatus

In order to evaluate the effect of the collisions between the atoms inside the beam, we need to consider the geometry of the experimental setup. A detailed description of the $2S$–$4P$ experiment in Garching is given in [1, 21]. For the calculation of the collisional shift, we use a simplified model, based on the actual geometry of the experiment (see figure 2).

According to this model, hydrogen atoms in the $1S$ state are emitted from a cryogenic circular nozzle with a temperature of $T = 5.8$ K. The atomic beam is collimated by several diaphragms, aligned along the $1S$–$2S$ two-photon excitation laser beam at 243 nm. After passing through the excitation region, where they can be excited to the $2S$ state, the atoms come into the $2S$–$4P$ spectroscopy region, in which they cross the 486 nm laser beam. A possible bias due to simultaneous irradiation of the $2S$ atoms by the $1S$–$2S$ laser beam during the $2S$–$4P$ spectroscopy is avoided by shuttering the $1S$–$2S$ laser beam with rate of 160 Hz. The $2S$–$4P$ excitation signal is detected via Ly-α and Ly-γ decays and recorded only in the periods when the $1S$–$2S$ laser beam is blocked. A multi-channel scaler separates the signal from the $2S$–$4P$ spectroscopy into several groups according to the delay between the beam blocking falling front and the photon detection. The velocity distribution of the atoms v_A strongly depends on the delay, since fast atoms pass the $2S$–$4P$ spectroscopy region earlier than slow ones.

The total flux of hydrogen atoms in our calculation is taken from the measured flow of the hydrogen gas into the apparatus during the $2S$–$4P$ measurement (approximately 1.8×10^{18} H_2 molecules per second). An estimate of the dissociation rate into hydrogen atoms can be obtained indirectly, via two independent methods, which independently indicate a fraction of atomic hydrogen on the order of 10%. The first estimate proceeds as follows. Upon a decrease in temperature from 20 to 5.8 K, the residual pressure near the nozzle is observed to decrease by more than a factor 10. Within a crude approximation, we can assume that molecular hydrogen, as opposed to atomic hydrogen, becomes solid in this temperature range and is left on the nozzle as ice, which means that about 90% of the gas remains in molecular form. Alternatively, we experimentally study how the amplitude $A(T)$ of the line changes as a function of temperature. Within a crude approximation, one would have $A(T) = N\,d(T)\,e(T)$, where N is the number of molecules, $d(T)$ is the dissociation ratio, and $e(T)$ is the excitation probability. If N is independent of temperature, and $e(T)$ is proportional to $1/T$ (see [22]), then the amplitudes of the lines at 5.8 and 300 K should be related to the corresponding dissociation rates as $A(5.8\,\mathrm{K})/A(300\,\mathrm{K}) \approx [d(5.8\,\mathrm{K})/d(300\,\mathrm{K})]\,[(5.8\,\mathrm{K})/(300\,\mathrm{K})]$. This estimate also is compatible with a dissociation rate not exceeding 10 %, and a flow of hydrogen atoms thus not exceeding 3.6×10^{17} atoms s^{-1}.

4.2. Analytic estimate for intra-beam collisions

It is interesting to note that the collisional shift can be estimated via a simple analytic calculation. We notice that the average velocity of the atoms leaving the nozzle in the case of a Maxwell distribution with temperature $T = 5.8$ K is about $v = 3\sqrt{\pi/8 \times k_B T/m_H} \approx 410$ m s^{-1}. If all the atoms are flying from a point-like source with a uniform angular distribution, the number of atoms crossing the sphere of radius L_1 can be estimated as $N = 4\pi\, L_1^2\, v\, \mathfrak{n}$, where $\mathfrak{n}$ is a number density of the atoms. From the flux $N = 3.6 \times 10^{17}$ atoms s^{-1}, one can estimate the concentration of ground-state hydrogen atoms in the atomic beam at a distance of about $L_1 = 16.4$ cm from the nozzle to be about $\mathfrak{n} = N/(4\pi\, L_1^2\, v) \approx 2.6 \times 10^{15}$ atoms m^{-3}. For $1S$–$4P_{3/2}$ collisions with a velocity of 410 m s^{-1}, the collisional shift cross-section is about $\sigma_\omega = -5.1 \times 10^{-17}$ rad m^2, which finally gives a shift $\omega_c/(2\pi) = \mathfrak{n}\, v\, \sigma_\omega/(2\pi) \approx -8.6$ Hz. We recall that for $4P_{1/2}$, the van der Waals potential is repelling, while for $4P_{3/2}$, it is attractive [14]. This result is close to the result of the Monte-Carlo simulations, confirming the possibility to neglect pressure-related effects on the current level of experimental uncertainty [1, 21].

4.3. Monte-Carlo calculation for intra-beam collisions

The simple analytic estimate given above can be criticized since we ignore the complicated spatial and velocity distributions of the hydrogen atoms. In order to take this into account, we use an approach based on a Monte-Carlo simulation. In the framework of this simulation, we consider the collisional shift caused by collisions with other atoms from the same beam. These can be in either the $1S$ or $2S$ state. For simplicity, we do not model a full lineshape of the $2S$–$4P$ spectroscopy, but restrict our evaluation to the collisional shift, equally weighted over the set of $2S$ atoms. For the computation of the excitation probability of the spectator atoms A in the delay window from, say, τ_1 to τ_2, we use an existing Monte-Carlo approach, described in [23, 24]. The origin points of trajectories of the hydrogen atoms in this simulation are seeded uniformly on the orifice of the nozzle, while the velocity vectors of these trajectories are seeded uniformly in the corresponding solid angle. The trajectories which do not pass all diaphragms are rejected. The program is also choosing a random absolute value of the velocity v_A of the atom according to a Maxwellian distribution, and the random position of the atom z_{off} on the z-axis, where the atom is located at the moment of shuttering the excitation light. The Monte-Carlo procedure discards the seeded trajectory if the atom does not fall into the delay window, characterized by the condition $\tau_1 < \tau < \tau_2$. Here, we designate as $\tau = (L_0 - z_{\mathrm{off}})/v_{Az}$ an individual delay of the atom A, where L_0 is the distance from the nozzle to the $2S$–$4P$ laser beam, and v_{Az} is the z component of the velocity of the atom. For all the atoms which fit into the delay window, we can compute the excitation probability ρ_{22} to the $2S$ state by integrating the optical Bloch equations from the moment of the beginning of trajectory to the moment when the light is shuttered off.

The result of the procedure described above is a set of random atomic trajectories described by the initial position $\vec{r}_{A0}$, the velocity vector $\vec{v}_A$ and the individual delay of the atom τ. For each trajectory, one computes the excitation probability to the $2S$ state ρ_{22}, and the position of the atom $\vec{r}_{\mathrm{col}}$, when it is crossing the $2S$–$4P$ laser beam. Random collisions with other atoms B in the vicinity of the point $\vec{r}_{\mathrm{col}}$ cause the intra-beam shift, where we assume that the modulus of $\vec{r}_{\mathrm{col}}$ is large against the distance of closest approach of the two atoms during the collision, i.e. large against the impact parameter b. This means that $|\vec{r}_{\mathrm{col}}| \gg |\vec{r}_A(t_{\mathrm{col}}) - \vec{r}_B(t_{\mathrm{col}})| \equiv b$, where t_{col} is the point in time of closest approach of the two atoms. The

weight for this averaging is the excitation probability of the atom A, which we denote as ρ_{22}.

The evaluation of the collisional shift of the atom A in the position $\vec{r}_{\rm col}$ with velocity $\vec{v}_A$ can be done via the cross-sections of the collisional shifts, computed by formula (32). In order to evaluate collision rates and velocities, we can describe our nozzle as a set of point-like sources of atoms B. Each source s with position $\vec{r}_s$ emits N_s atoms per second with a velocity distribution $p(v_B)$ and an angular distribution $\Psi(\hat{e})$, where $\hat{e}$ is a unit vector representing direction. We assume that atomic trajectories are straight during the $1S$–$2S$ excitation phase, so that $\hat{e}$ can be expressed as

$$\hat{e} = \frac{\vec{r}_{\rm col} - \vec{r}_s}{|\vec{r}_{\rm col} - \vec{r}_s|}. \tag{41}$$

For most atoms contributing to the experimentally observed line shape, the assumption of a straight trajectory of the atoms during the $1S$–$2S$ excitation (which is of course different from the subsequent $2S$–$4P$ excitation) is valid since the probability of the collision with a small deflection angle (which allows the atom to pass through the front and rear diaphragms) is quite small. For example, our estimation shows, that the fraction of atoms, which can be deflected by the angle between 10^{-4} and 10^{-1} rad, is less than 10^{-3}. In our experimental geometry, that implies that either, the atoms in the atomic beam in the $2S$–$4P$ spectroscopy region come to this region from the nozzle without a strong deviation from the straight-line trajectory, or they do not get there at all.

A remark is in order, which is relevant especially for the $2S$–$4P$ excitation region, because of the large C_6 coefficients governing atoms in the excited P state. As we show in appendix C, it is interesting to observe that the assumption that the trajectory of the atom is close to a straight line during the collision, actually is not fulfilled in the complete range of impact parameters relevant to our calculation. When the impact parameter is close to a 'deflection radius', which for our geometry is close to the Weisskopf radius, then the trajectories of the colliding particles are strongly deflected. In this case, the problem of the collisional shift should be considered with a full account of the experimental geometry. In the setup of the Garching $2S$–$4P$ experiment, the atoms, deflected in the region of $2S$–$4P$ spectroscopy, remain in a spatial region where the emitted decay photons could be registered by the detector, upon decay, in the form of Lyman-α (after quenching) and Lyman-γ photons (from the $4P$ state).

Experimentally, if the $2S$ atom is kicked out of the beam, then it will hit the wall of the detector 'box'. With a high probability, a collision with the wall leads to a quenching of the $2S$ state, due to the interaction of the atom with the surface of the grounded conductor, and emission of a Lyman-α photon. (In our experiment, we actually do not detect the photons, but the photoelectrons, which they kick out from the walls, as described in [1].)

When $2S$ (or, conceivably, $4P$) atoms are kicked out of the beam by collisions with small impact parameters, they do so irrespective of the frequency of the spectroscopy laser. In other words, if the $2S$ atom leads to an event registered by the detector, regardless of the state of $2S$–$4P$ laser, the atom could only contribute to the constant background, which is eliminated by our fitting procedure [1]. Only the atoms with a small deflection angle (less than 10^{-1} rad) contribute to the observed resonance line shape. The latter escape from the detector undetected if the $2S$–$4P$ laser is off-resonance and are detected via decay from the $4P$ state if the $2S$–$4P$ laser is in resonance. In our Monte Carlo simulation, we assume that the trajectories of the colliding atoms are straight, and ignore the possibility of a large deflection from the straight-line trajectory. Thus, we very likely overestimate the observed collisional shift, because we also take into consideration the atoms with a large deflection angle; these should otherwise be ignored because they only contribute to the background. In consequence, a Monte Carlo simulation with straight trajectories during the $2S$–$4P$ excitation can be used as an estimate of an upper limit of the collisional shift.

The number density of atoms B with velocities in the interval $(v_B,\ v_B + {\rm d}v_B)$, created by the source s in the point $\vec{r}_{\rm col}$, can be evaluated as

$$\begin{aligned} {\rm d}n_{sv} = {} & \frac{N_s}{4\pi v_B\,|\,\vec{r}_{\rm col} - \vec{r}_s\,|^2}\Psi\left(\frac{\vec{r}_{\rm col} - \vec{r}_s}{|\,\vec{r}_{\rm col} - \vec{r}_s\,|}\right) \\ & \times \Xi(\vec{r}_s,\,\vec{r}_{\rm col})\; p(v_B)\;{\rm d}v_B, \end{aligned} \tag{42}$$

where $\Xi(\vec{r}_s,\,\vec{r}_{\rm col})$ is a filtering function, which is equal to unity if the trajectory, starting at $\vec{r}_s$ and heading towards $\vec{r}_{\rm col}$, passes all diaphragms installed in our experiment, and zero if not. The relative velocity of the atoms A and B is

$$\vec{v}_{\rm col} = \vec{v}_A - \vec{v}_B = \vec{v}_A - v_B\,\frac{\vec{r}_{\rm col} - \vec{r}_s}{|\vec{r}_{\rm col} - \vec{r}_s|}, \tag{43}$$

and so, the infinitesimal frequency shift ${\rm d}\omega_{sv}$ caused by the source s and velocity component $(v_B,\ v_B + {\rm d}v_B)$ is:

$$\begin{aligned} {\rm d}\omega_{sv} = {} & \frac{N_s}{4\pi v_B\,|\,\vec{r}_{\rm col} - \vec{r}_s\,|^2}\;\Psi\left(\frac{\vec{r}_{\rm col} - \vec{r}_s}{|\,\vec{r}_{\rm col} - \vec{r}_s\,|}\right) \\ & \times \Xi(\vec{r}_s,\,\vec{r}_{\rm col})\; p(v_B)\;{\rm d}v_B \\ & \times \left|\vec{v}_A - v_B\frac{\vec{r}_{\rm col} - \vec{r}_s}{|\,\vec{r}_{\rm col} - \vec{r}_s\,|}\right| \\ & \times \sigma_\omega\left(\left|\,\vec{v}_A - v_B\frac{\vec{r}_{\rm col} - \vec{r}_s}{|\,\vec{r}_{\rm col} - \vec{r}_s\,|}\,\right|\right). \end{aligned} \tag{44}$$

The angular distribution Ψ, for practial calculations, is taken proportional to the $\cos(\theta)$, where the θ is the angle between the normal vector to the surface of the nozzle outlet and the atomic trajectory. This choice is motivated by Lambert's cosine law, which is well known for ideal diffusive radiators. In order to write this probability distribution function explicitly, we can introduce another angle φ so that θ and φ define a spherical coordinate system, whose z axis points away from the point of the source in direction of the normal vector to the nozzle surface. In this coordinate system, the probability distribution Ψ can be written as

$$\Psi(\theta,\,\varphi) = \cos(\theta)\sin(\theta)/\pi, \tag{45}$$

which is normalized to

$$\int_0^{2\pi} \mathrm{d}\varphi \int_0^{\pi/2} \mathrm{d}\theta\, \Psi(\theta, \varphi) = 1. \tag{46}$$

Indeed, for our nozzle, the relevant angular ranges are $0 < \theta < \pi/2$ and $0 < \varphi < 2\pi$.

In order to compute the collisional shift of the individual atom A, this function should be integrated over all the velocities v_B and all the sources of atoms s. It is clear that any attempt at an analytic computation of this integral would be hopeless even in simple cases. However, we can use the Monte-Carlo method with good effect. It is advantageous to restrict possible values of the velocity v_B to an interval from zero to $v_{\max}$, where $v_{\max}$ is a velocity chosen to be bigger than the velocity of most of our atoms. One then needs to calculate the average value of the function

$$\begin{aligned}\Omega_{sv} = \frac{1}{N_s}\frac{\mathrm{d}\omega_{sv}}{\mathrm{d}v_B} = {} & \frac{1}{4\pi v_B |\vec{r}_{\mathrm{col}} - \vec{r}_s|^2} \\ & \times \Psi\left(\frac{\vec{r}_{\mathrm{col}} - \vec{r}_s}{|\vec{r}_{\mathrm{col}} - \vec{r}_s|}\right) \Xi\,(\vec{r}_s, \vec{r}_{\mathrm{col}})\, p(v_B) \\ & \times \left| \vec{v}_A - v_B \frac{\vec{r}_{\mathrm{col}} - \vec{r}_s}{|\vec{r}_{\mathrm{col}} - \vec{r}_s|} \right| \\ & \times \sigma_\omega\left(\left| \vec{v}_A - v_B \frac{\vec{r}_{\mathrm{col}} - \vec{r}_s}{|\vec{r}_{\mathrm{col}} - \vec{r}_s|} \right| \right).\end{aligned} \tag{47}$$

For this averaging, we should seed the velocity of the atom v_B according to a uniform distribution, since the function Ω_{sv} contains the properly normalized probability density function $p(v_B)$. The sources of the atom can be seeded with a weight determined according to their flux N_s, which practically means that in each Monte-Carlo run, we can randomly choose, as the point of origin of atom B, a specific point $\vec{r}_s$ on the nozzle orifice. The total shift can be evaluated as:

$$\omega_{\mathrm{col}} = \sum_s \int_0^{v_{\max}} \mathrm{d}\omega_{sv} \approx N_{\mathrm{tot}}\, v_{\max}\, \langle \Omega_{sv} \rangle_{\mathrm{MC}}\,, \tag{48}$$

where N_{tot} is a sum of fluxes of all the sources, and $\langle \cdots \rangle_{\mathrm{MC}}$ represents a Monte-Carlo averaging. Notice, that in this approach to the intra-beam collisional shift, we do not necessarily need to use discrete sources of the perturbing atoms. The sources can be distributed on some surface or even in an extended volume. For the purpose of our evaluation, we assume that sources are uniformly distributed on the orifice of the nozzle.

A particular effect which should be considered in the $2S$–$4P$ experiment, concerns the possibility to collide with another $2S$ atom in the beam. In order to take this effect into account, we compute the probability ρ_{22B} of excitation of each atom B. We can use the fact that the individual delay of atom B must exactly coincide with the individual delay τ of the atom A. If the seeded velocity of atom B satisfies the condition $v_{Bz} > L_0/\tau$, then atom B leaves the nozzle after the light was shuttered off, so this atom cannot be excited to the $2S$ state and $\rho_{22B} = 0$. If $v_B < L_0/\tau$, then atom B can be excited to the $2S$ state with a probability, which can be computed by an integration of the optical Bloch equations.

We also need to take into account, that the $1S$–$2S$ laser beam excites only atoms in the $1S(F = 0)$ state, since the transition $1S(F = 1) \to 2S(F = 1)$ is not in resonance with the $1S$–$2S$ laser beam. According to statistical weight, the probability that the atom originates in a state $F = 0$ is $1/4$, so we should multiply the result of the integration of the Bloch equations by the factor $1/4$. Thus, we can separate the collisional shift into two parts—collisions with $1S$ atoms and collisions with $2S$ atoms—by averaging two different functions:

$$\begin{aligned}\Omega_{sv}^{1S} = {} & \frac{1 - \rho_{22B}}{4\pi v_B |\vec{r}_{\mathrm{col}} - \vec{r}_s|^2} \Psi\left(\frac{\vec{r}_{\mathrm{col}} - \vec{r}_s}{|\vec{r}_{\mathrm{col}} - \vec{r}_s|}\right) \\ & \times \Xi(\vec{r}_s, \vec{r}_{\mathrm{col}})\, p(v_B) \\ & \times \left| \vec{v}_A - v_B \frac{\vec{r}_{\mathrm{col}} - \vec{r}_s}{|\vec{r}_{\mathrm{col}} - \vec{r}_s|} \right| \\ & \times \sigma_\omega^{1S}\left(\left| \vec{v}_A - v_B \frac{\vec{r}_{\mathrm{col}} - \vec{r}_s}{|\vec{r}_{\mathrm{col}} - \vec{r}_s|} \right| \right),\end{aligned} \tag{49}$$

$$\begin{aligned}\Omega_{sv}^{2S} = {} & \frac{\rho_{22B}}{4\pi v_B |\vec{r}_{\mathrm{col}} - \vec{r}_s|^2} \Psi\left(\frac{\vec{r}_{\mathrm{col}} - \vec{r}_s}{|\vec{r}_{\mathrm{col}} - \vec{r}_s|}\right) \\ & \times \Xi(\vec{r}_s, \vec{r}_{\mathrm{col}})\, p(v_B) \\ & \times \left| \vec{v}_A - v_B \frac{\vec{r}_{\mathrm{col}} - \vec{r}_s}{|\vec{r}_{\mathrm{col}} - \vec{r}_s|} \right| \\ & \times \sigma_\omega^{2S}\left(\left| \vec{v}_A - v_B \frac{\vec{r}_{\mathrm{col}} - \vec{r}_s}{|\vec{r}_{\mathrm{col}} - \vec{r}_s|} \right| \right).\end{aligned} \tag{50}$$

The cross-sections of the shift σ_ω^{nS}, with $n = 1, 2$, can be computed using formula (32). The C_6 coefficient for $1S$ collisions should be averaged over all possible hyperfine sublevels of the $1S$ state, while the C_6 coefficient for the $2S$ atoms should take into account only $2S$ atoms in the $F = 0$ state. The C_6 coefficients used for our simulation together with the results of the calculation are given in table 3. It is instructive to perform a similar calculation, for the ongoing $2S$–$6P$ experiment in the same apparatus. Corresponding results are given in table 4.

4.4. Collisions with background gas

Here, we consider the pressure shift caused by collisions with the background gas. A precise calculation of this shift has no practical interest because of the unknown fraction of atomic hydrogen in the background gas, and fluctuations of the pressure in the $2S$–$4P$ spectroscopy region caused by cryo-pump working cycles. Thus, our goal is to conservatively estimate the shift from beam-background collisions, assuming that the effect from the molecules is less than or comparable to that caused by the atomic hydrogen in the background gas. In fact, because of a much smaller C_6 coefficients for the atom-molecule as compared to the atom-atom collisions (see section 5 of [14]), this assumption should be well justified. The calculation described below takes only the effect of collisions with atomic hydrogen into account. In fact, we can easily do the calculation analytically under the assumption that the velocities of the atoms in the atomic beam are much smaller than the velocities of the background gas.

Table 3. Results are given for a Monte-Carlo evaluation of the total intra-beam collisional shift $f(X) = \omega_{\rm col}$, as defined in equation (48), where X is a delay interval, as discussed in the text. The data are relevant for the $2S$–$4P$ experiment, and the corresponding C_6 coefficients. The C_6 coefficient is given in atomic units (i.e. in units of $E_h\, a_0^6$), while the frequency shifts are given in Hz. The notation $f(\tau_1 - \tau_2) = \omega_{\rm col}(\tau_1 - \tau_2)/(2\pi)$ denotes a frequency shift in Hz, computed for the delay window from τ_1 to τ_2, i.e. for atoms that arrive within the given delay interval after the beam blocking. The values of τ_i are given in μs. The uncertainty of the Monte-Carlo evaluation is on the order of 3%.

System	$1S$–($2S$–$4P_{1/2}$)	$2S$–($2S$–$4P_{1/2}$)	$1S$–($2S$–$4P_{3/2}$)	$2S$–($2S$–$4P_{3/2}$)
C_6 (a.u.)	1.296×10^5	9.090×10^9	-5.921×10^5	3.296×10^9
f(10–60) (Hz)	5.4	0.92	−10.0	0.61
f(60–110) (Hz)	5.3	0.75	−9.8	0.50
f(110–160) (Hz)	5.1	0.61	−9.3	0.41
f(160–210) (Hz)	4.7	0.48	−8.7	0.32
f(210–260) (Hz)	4.6	0.35	−8.5	0.24
f(260–310) (Hz)	4.5	0.25	−8.2	0.17
f(310–410) (Hz)	4.5	0.17	−8.3	0.11
f(410–610) (Hz)	4.8	0.076	−8.8	0.051
f(610–810) (Hz)	5.2	0.024	−9.6	0.016
f(810–2560) (Hz)	6.1	0.005	−11.3	0.003

Table 4. Results are given for a Monte-Carlo evaluation of the intra-beam collisional shift $f(X) = \omega_{\rm col}$, as defined in equation (48), with X denoting a delay interval. Here, we consider the $2S$–$6P$ experiment and the corresponding C_6 coefficients. The C_6 coefficients are given in atomic units and the frequency shifts in Hz. The notation $f(\tau_1 - \tau_2) = \omega_{\rm col}(\tau_1 - \tau_2)/(2\pi)$ means a frequency shift in Hz, computed for the delay window from τ_1 to τ_2, i.e. for atoms that arrive within the given delay interval after the beam blocking. The values of τ_i are given in μs. The uncertainty of the Monte-Carlo evaluation is on the order of 3%.

System	$1S$–($2S$–$6P_{1/2}$)	$2S$–($2S$–$6P_{1/2}$)	$1S$–($2S$–$6P_{3/2}$)	$2S$–($2S$–$6P_{3/2}$)
C_6 (a.u.)	2.074×10^4	4.280×10^{10}	-1.336×10^5	2.918×10^{10}
f(10–60) (Hz)	2.6	1.7	−5.5	1.5
f(60–110) (Hz)	2.6	1.4	−5.4	1.2
f(110–160) (Hz)	2.4	1.1	−5.2	0.99
f(160–210) (Hz)	2.3	0.89	−4.9	0.76
f(210–260) (Hz)	2.2	0.66	−4.6	0.56
f(260–310) (Hz)	2.2	0.48	−4.6	0.41
f(310–410) (Hz)	2.2	0.31	−4.6	0.26
f(410–610) (Hz)	2.3	0.13	−4.9	0.12
f(610–810) (Hz)	2.5	0.05	−5.3	0.04
f(810–2560) (Hz)	2.9	0.009	−6.2	0.008

The general setting is as follows. We consider an atomic beam, at a temperature of about 5.8 K, with hydrogen atoms inside the beam being perturbed by a 300 K background gas, consisting of atomic hydrogen in the ground state. The $1S$–$2S$ excitation probability depends on the velocity of the atom and the chosen experimental delay group, but for all delay groups, the average velocity of $2S$ atoms in the beam is less than $300\ \mathrm{m\,s^{-1}}$. The thermal velocity of the background gas atoms is about $3\ \mathrm{km\,s^{-1}}$, which means that we can neglect the movement of the spectator atom A in comparison with the perturber atom B. Thus, the velocity of the collision is $v = |\vec{v}_A - \vec{v}_B| \approx v_B$. The pressure shift and the pressure broadening can be calculated from the known cross-sections:

$$\omega_c = \mathfrak{n} \int_0^\infty \sigma_\omega^{(6)}(v) v\, P(v) \mathrm{d}v,$$
$$\gamma_c = \mathfrak{n} \int_0^\infty \sigma_\gamma^{(6)}(v) v\, P(v) \mathrm{d}v, \qquad (51)$$

where $P(v)$ is the velocity distribution of the background gas and $\mathfrak{n}$ is the number density of $1S$ atoms. For our estimation, we can use a Maxwellian velocity distribution, which reads as follows,

$$P(v) = \sqrt{\frac{2}{\pi}} \left(\frac{m}{k_B T}\right)^{3/2} v^2 \exp\left(-\frac{m v^2}{2 k_B T}\right), \qquad (52)$$

where m is a mass of background gas particle (hydrogen atom), k_B is a Boltzmann constant, $T = 300$ K is a background gas temperature.

Putting $\sigma_\omega^{(6)}(v) = \xi_\omega^{(6)} v^{-2/5}$ and $\sigma_\gamma^{(6)}(v) = \xi_\gamma^{(6)} v^{-2/5}$, the integral (51) can be computed analytically with the result

$$\omega_c = \frac{2^{13/10}}{\sqrt{\pi}} \Gamma\left(\frac{9}{5}\right) \mathfrak{n}\, \xi_\omega^{(6)} \left(\frac{k_B T}{m}\right)^{3/10}$$
$$= 1.293\,88 \times \mathfrak{n}\, \xi_\omega^{(6)} \left(\frac{k_B T}{m}\right)^{3/10}, \qquad (53)$$

$$\gamma_c = 1.293\,88 \times \mathfrak{n}\,\xi_\gamma^{(6)} \left(\frac{k_B T}{m}\right)^{3/10}. \tag{54}$$

We recall that both the $\xi_\omega^{(6)}$ and $\xi_\gamma^{(6)}$ are proportional to $C_6^{2/5}$. Consequently, both ω_c and γ_c are also proportional to $C_6^{2/5}$.

At a temperature of 300 K and a pressure less than 10^{-8} mbar, the density of the background gas does not exceed $2.4 \times 10^{14}\ \mathrm{m}^{-3}$. Under these conditions, the background shift in the $2S$–nP experiments (with $n = 4, 6$) does not exceed the following values:

$$\omega_c(1S - 4P_{1/2}) = 2\pi \times 1.24\ \mathrm{Hz},$$
$$\gamma_c(1S - 4P_{1/2}) = 2\pi \times 1.70\ \mathrm{Hz}, \tag{55a}$$
$$\omega_c(1S - 4P_{3/2}) = -2\pi \times 2.34\ \mathrm{Hz},$$
$$\gamma_c(1S - 4P_{3/2}) = 2\pi \times 3.22\ \mathrm{Hz}, \tag{55b}$$
$$\omega_c(1S - 6P_{1/2}) = 2\pi \times 0.57\ \mathrm{Hz},$$
$$\gamma_c(1S - 6P_{1/2}) = 2\pi \times 0.78\ \mathrm{Hz}, \tag{55c}$$
$$\omega_c(1S - 6P_{3/2}) = -2\pi \times 1.29\ \mathrm{Hz},$$
$$\gamma_c(1S - 6P_{3/2}) = 2\pi \times 1.78\ \mathrm{Hz}. \tag{55d}$$

The quantities ω_c and γ_c in equations (55*a*)–(55*d*) are the hyperfine-structure averages of the shifts. For both the frequency shift as well as the broadening, the averaging scheme outlined in equations (40) has been used,

$$\omega_c \sim \langle |C_6|^{2/5} \rangle, \quad \gamma_c \sim \langle |C_6|^{2/5} \rangle. \tag{56}$$

The importance of the proper averaging procedure is discussed in appendix B.

5. Conclusions

In this paper, we have outlined a procedure for the calculation of pressure shifts in the Garching $2S$–$4P/6P$ experiments; however, similar approaches can be used in other modern high-precision spectroscopic atomic-beam experiments. The treatment is based on the impact approximation (section 2), in which the phase and frequency shifts in the collisions are modeled on the basis of 'quasi-instantaneous' impacts onto the spectator atoms, by colliding with perturber atoms. The basis for the calculation of the collisional shifts and broadenings is discussed in section 3. An integration of the frequency shift, and of the pressure broadening, over the impact parameter b, leads to results for the frequency-shift and broadening cross sections which are proportional to $|C_6|^{2/5}$, where C_6 is the van der Waals coefficient (see section 3.3). The data in table 2, with appropriate modifications of the hyperfine averages [12–14], could be used for the description of pressure shifts in $1S$–nS ($n = 2, 3, 4$) and $2S$–nP experiments ($n = 4, 6$).

An application of the developed formalism to recent and planned $2S$–$4P$ and $2S$–$6P$ experiments is discussed in section 4. After a discussion of the experimental apparatus in section 4.1, an analytic estimate of the frequency shift is presented in section 4.2, and a more elaborate Monte Carlo simulation is discussed in section 4.3. Using the Monte-Carlo simulation, we can implement the computation of the pressure shifts for the delayed measurement scheme used in the Garching experiment. The collisional velocity spectrum and the number of the $2S$ atoms strongly depend on the delay [1, 4, 5]. Our approach allows us to take into account all those effects.

Finally, in addition to intra-beam collisions, the effect of beam-background collisions is discussed in section 4.4. The beam-background collisions can be treated in the approximation that the velocity of the particles in the beam is much smaller than the average velocity of background gas particles. Numerical results for intra-beam, and beam-background collisional shifts, are given in tables 3 and 4, respectively.

For the $2S$–$4P$ experiment [1], it is shown that the possible shift in the current configuration of the experiment is on the order of magnitude of 10Hz, which is two orders of magnitude smaller than the current uncertainty of the experiment. In order to put this number into perspective, we observe that the leading uncertainties of the $2S$–$4P$ experiment [1] are the uncertainty of the Doppler shift compensation of 2.9 kHz, the quantum interference shift compensation of 0.33 kHz, and light force shifts of 0.4 kHz. The first-order Doppler effect also causes a broadening of the observed lineshape on the level of 10 MHz. While the collisional effects are thus smaller than other sources of uncertainty in the experiment, they require a rather subtle analysis, as discussed here. The model presented in this work allows us also to estimate the collisional shift for the ongoing $2S$–$6P$ experiments in the Garching laboratory. In view of data presented in table 2, the approach can easily be generalized to other transitions.

Acknowledgments

The authors acknowledge insightful conversations with Professor T W Hänsch, Th Udem and V Debierre. This research has been supported by the National Science Foundation (Grant PHY–1710856), as well as the Missouri Research Board. NK acknowledges support from DFG-RFBR grants (HA 1457/12-1 and 17-52-12016). AM acknowledges support from the Deutsche Forschungsgemeinschaft (DFG grant MA 7628/1-1).

Appendix A. First-order van der Waals shifts and pressure shift

We aim to show that the first-order van der Waals long-range interaction, proportional to $1/R^3$, does not contribute to the pressure shift of an atomic transition after proper averaging over the impact parameters $\vec{b}$ and the collisional velocities $\vec{v}$. To this end, we first recall and rewrite equation (9) as

$$\langle \mathrm{e}^{-\mathrm{i}(\psi(t)-\psi(t-\tau))} \rangle = \exp\left(-\tau \int_{-\infty}^{\infty} a(\phi)[1-\mathrm{e}^{-\mathrm{i}\,\phi}]\,\mathrm{d}\phi \right)$$
$$= \mathrm{e}^{-\theta(v)\tau}, \tag{A.1}$$

where

$$\theta(v) = \int_{-\infty}^{\infty} a(\phi)\,[1 - \mathrm{e}^{-\mathrm{i}\,\phi}]\,\mathrm{d}\phi$$
$$= 2\pi\,\mathfrak{n} \int_{-\infty}^{\infty} v\,b\,[1 - \mathrm{e}^{-\mathrm{i}\,\phi}]\,\mathrm{d}b. \tag{A.2}$$

In equation (A.2), we have used equation (24) to eliminate $a(\phi)\,\mathrm{d}\phi$. For any velocity distribution $P(v)$, the quantity

$$\theta = \int_0^\infty \theta(v) P(v)\,\mathrm{d}v \tag{A.3}$$

is the impact-broadening operator (also called the θ-operator, see [15]). It is called an 'operator' because, as we shall see, the phase shift ϕ can depend on dipole-operator matrix elements evaluated for the two atoms. Being inspired by equation (23), where a directionally averaged interaction, proportional to $1/R^n$, was considered, one can go 'one step back' and consider a general interaction $U(t, \vec{R})$,

$$\phi = \phi(v, b) = \frac{1}{\hbar}\int_{-\infty}^{\infty} \mathrm{d}t\; U(\vec{R}(t, \vec{v}, \vec{b})), \tag{A.4}$$

where $\vec{R}(t) = \vec{R}(t, \vec{v}, \vec{b}) = \vec{b} + \vec{v}\,t$ describes the trajectory of the atom with impact parameter vector $\vec{b}$, which we choose so that the closest point of approach is reached at $t = 0$ (see equation (4) of [20]). This, in particular, implies that $\vec{v}\cdot\vec{b} = 0$. Consequently, the θ-operator can be expressed as

$$\theta = 2\pi\,\mathfrak{n}\int_0^\infty vP(v)\int_0^\infty b[1 - \exp\left(-\frac{\mathrm{i}}{\hbar}\int_{-\infty}^{\infty} U(\vec{R}(t, \vec{v}, \vec{b})\,\mathrm{d}t\right)]\,\mathrm{d}v\,\mathrm{d}b. \tag{A.5}$$

The resonance dipole–dipole interaction is given by

$$\begin{aligned} U(t, \vec{v}, \vec{b}) &= \frac{1}{4\pi\epsilon_0} \times \frac{\vec{d}_A(t)\cdot\vec{d}_B(t) - 3(\vec{d}_A(t)\cdot\hat{R}(t))(\vec{d}_B(t)\cdot\hat{R}(t))}{||\vec{R}||^3} \\ &= \frac{1}{4\pi\epsilon_0}\left[\frac{\vec{d}_A(t)\cdot\vec{d}_B(t)}{(b^2 + v^2t^2)^{3/2}} - 3\,\frac{[\vec{d}_A(t)\cdot(\vec{b} + \vec{v}\,t)][\vec{d}_B(t)\cdot(\vec{b} + \vec{v}\,t)]}{(b^2 + v^2t^2)^{5/2}}\right]. \end{aligned} \tag{A.6}$$

where $\vec{d}_i(t) = e\,\vec{r}_i(t)$ is the electric dipole operator for the atom $i = A, B$ and $\hat{R} = \vec{R}/||\vec{R}||$ is the unit vector along $\vec{R}(t)$. The pressure shift is given by the imaginary part of the average value of θ-operator. For resonance dipole–dipole interaction, we have [20]

$$\sigma_\omega = \mathrm{Im}\langle\alpha|\,\theta|\alpha\rangle, \quad \sigma_\gamma = \mathrm{Re}\langle\alpha|\,\theta|\alpha\rangle. \tag{A.7}$$

Here, $|\alpha\rangle$ is the ket corresponding to the reference state of the two-atom system. Note that the operators $\vec{d}_i(t)$ in equation (A.6) enter the interaction Hamiltonian in the interaction picture, i.e. they acquire a time dependence due to the time dependence of the atomic states involved in the transition. (Strictly speaking, the exponential in equation (A.6) is time-ordered, in the sense of an S-matrix element.) The question now is whether the first-order (in the van der Waals interaction) effect could lead to a frequency shift. To this end, we observe that a potential first-order effect is relevant only in the space of perfectly degenerate states of the two-atom system, which can be reached via a dipole transition. Within this space, however, we can replace

$$\vec{d}_i(t) = \exp(\mathrm{i}H_0\,t)\,d_i\,\exp(-\mathrm{i}H_0\,t) \to \vec{d}_i, \tag{A.8}$$

because the operator acts in a degenerate subspace of H_0, which is the unperturbed Hamilton operator of the atom. We thus get, to first order in perturbation theory (see equation (5) of [20]),

$$\begin{aligned} 1 - \exp\left(-\frac{\mathrm{i}}{\hbar}\int_{-\infty}^{\infty}\mathrm{d}t\; U(t, \vec{b}, \vec{v})\right) &\approx \frac{2\mathrm{i}}{4\pi\epsilon_0\,\hbar v\,b^2}[\vec{d}_A\cdot\vec{d}_B - 2(\vec{d}_A\cdot\hat{b})(\vec{d}_B\cdot\hat{b}) \\ &\quad - (\vec{d}_A\cdot\hat{v})(\vec{d}_B\cdot\hat{v})], \end{aligned} \tag{A.9}$$

where $\hat{b}$ and $\hat{v}$ are the unit vectors in the directions of the vectors $\vec{b}$ and $\vec{v}$. The average over angles of the scalar product $(\vec{d}_A\cdot\hat{x})(\vec{d}_B\cdot\hat{x})$ is given as

$$\langle(\vec{d}_A\cdot\hat{x})(\vec{d}_B\cdot\hat{x})\rangle = \frac{1}{3}\vec{d}_A\cdot\vec{d}_B. \tag{A.10}$$

As a result, the pressure shift in the resonance dipole–dipole interaction, in first-order perturbation theory, i.e. the average of the quantity

$$\vec{d}_A\cdot\vec{d}_B - 2(\vec{d}_A\cdot\hat{b})(\vec{d}_B\cdot\hat{b}) - (\vec{d}_A\cdot\hat{v})(\vec{d}_B\cdot\hat{v}), \tag{A.11}$$

vanishes after angular averaging over the directions of $\vec{b}$, and of $\vec{v}$. Note that the necessity of taking this average has been implied, but not explicitly written, in equation (A.3). The same approach is followed in [20].

Appendix B. Averaging the cross sections

For reference, we give some unified formulas which illustrate the averaging procedure outlined in the discussion surrounding equation (40), and the formulas for the cross sections given in equations (32)–(33*b*). Recall equations (53) and (54) for ω_c and γ_c and substitute $\xi_\omega^{(6)}$ and $\xi_\gamma^{(6)}$ from equations (32). we have

$$\begin{aligned} \omega_c &= -\frac{3^{2/5}\sqrt{5-\sqrt{5}}\;\Gamma\left(\frac{3}{5}\right)\Gamma\left(\frac{9}{5}\right)\pi^{9/10}}{2^{7/5}} \times \mathfrak{n}\left(\frac{k_BT}{m}\right)^{3/10}\mathrm{sgn}(C_6)\left(\frac{|C_6|}{\hbar}\right)^{2/5} \\ &= -3.799\;13\;\mathfrak{n}\left(\frac{k_BT}{m}\right)^{3/10}\mathrm{sgn}(C_6)\left(\frac{|C_6|}{\hbar}\right)^{2/5}, \end{aligned} \tag{B.1}$$

$$\begin{aligned} \gamma_c &= -\frac{3^{2/5}(\sqrt{5}+1)\Gamma\left(-\frac{2}{5}\right)\Gamma\left(\frac{9}{5}\right)\pi^{9/10}}{2^{9/10}\times 5} \times \mathfrak{n}\left(\frac{k_BT}{m}\right)^{3/10}\left(\frac{|C_6|}{\hbar}\right)^{2/5} \\ &= 5.229\;06\;\mathfrak{n}\left(\frac{k_BT}{m}\right)^{3/10}\left(\frac{|C_6|}{\hbar}\right)^{2/5}. \end{aligned} \tag{B.2}$$

It is clear from equations (B.1) and (B.2) that both the pressure shift and the broadening cross-section depend on C_6 and T according to a functional dependence of the form $|C_6|^{2/5}$ and

$T^{3/10}$. The average shifts and the broadening can be written as

$$\omega_c = \kappa_\omega \langle |C_6|^{2/5} \rangle, \quad \gamma_c = \kappa_\gamma \langle |C_6|^{2/5} \rangle, \tag{B.3}$$

where

$$\kappa_\omega = -3.799\ 13\ \mathfrak{m} \left(\frac{k_B T}{m} \right)^{3/10} \mathrm{sgn}(C_6)\ \hbar^{-2/5}, \tag{B.4}$$

$$\kappa_\gamma = 5.229\ 06\ \mathfrak{m} \left(\frac{k_B T}{m} \right)^{3/10} \hbar^{-2/5}, \tag{B.5}$$

and the $\langle |C_6|^{2/5} \rangle$ average is defined in equation (40). The cross sections are now given as

$$\omega_c = \kappa_\omega \frac{1}{\mathbb{M}} \sum_j \mathfrak{m}_j (|C_6^{(j)}|)^{2/5},$$
$$\gamma_c = \kappa_\gamma \frac{1}{\mathbb{M}} \sum_j \mathfrak{m}_j (|C_6^{(j)}|)^{2/5}. \tag{B.6}$$

Keeping in mind that almost all atoms in the background are in the $1S$ state, we obtain the pressure-shift ω_c and the pressure-broadening γ_c for $1S$–$4P_J$ and $1S$–$6P_J$ transitions as given in Eqs (55*a*)–(55*d*) above. One should, however, note that

$$\langle |C_6|^{2/5} \rangle = \frac{1}{\mathbb{M}} \sum_j \mathfrak{m}_j\, |C_6^{(j)}|^{2/5}$$
$$\neq \left(\frac{1}{\mathbb{M}} \sum_j \mathfrak{m}_j\, |C_6^{(j)}| \right)^{2/5} = \langle |C_6| \rangle^{2/5}. \tag{B.7}$$

Numerically, calculations show that for the atomic systems under consideration here, the difference between the two averaging procedures is relatively small but significant.

Appendix C. Deflection radius

We assume that $R(t)$ is the time-dependent distance between the atoms, where b is the impact parameter. Then, the distance-dependent energy shift E and the force F can be expressed as follows (see equations (17*a*) and (19)),

$$E = -\frac{C_6}{R^6}, \quad F = -\frac{\partial E}{\partial R} = -6\,\frac{C_6}{R^7},$$
$$R(t) = \sqrt{(v\,t)^2 + b^2}\,. \tag{C.1}$$

By Newton's first law, in nonrelativistic approximation, we can write the transverse acceleration $a_\perp(t)$ and the transverse velocity $v_\perp(t)$ as

$$a_\perp(t) = \frac{F \cos\vartheta}{m_\mathrm{H}}, \quad v_\perp(t) = \int a_\perp(t)\, \mathrm{d}t,$$
$$\cos\vartheta = \frac{b}{\sqrt{(v\,t)^2 + b^2}}, \tag{C.2}$$

where m_H is the mass of the hydrogen atom, approximately equal to the proton mass. The modulus of the final transverse velocity after the collision is

$$v_\infty = \left| \int_{-\infty}^{\infty} a_\perp(t)\, \mathrm{d}t \right| = \frac{15\pi}{8} \frac{C_6}{b^6\, m_\mathrm{H}\, v}. \tag{C.3}$$

The deflection angle α is given by the relation

$$\tan\alpha = \frac{v_\infty}{v} = \frac{15\pi}{8} \frac{C_6}{b^6\, m_\mathrm{H}\, v^2}. \tag{C.4}$$

A quick calculation with $R = 100\, a_0$ and $v = 300$ m/s shows that the deflection angle is of the order of about 10^{-2} rad and can thus fully be neglected for $C_6 = 10^5$ a.u., i.e. for $4P$–$1S$ collisions (see section 3 of [14]), but the atom is fully kicked out of its path for $C_6 = 10^9$ a.u., which is the relevant range for $4P$–$2S$ collisions (see section 4 of [14]). As explained here in section 4, atoms which are kicked out from the beam only contribute to the experimental background. Yet, as table 3 shows, the contribution of $4P$–$2S$ collisions to the collisional frequency shift is much smaller than that of $4P$–$1S$, so that an over-estimation of the former has negligible effect on the total estimate of the collisional frequency shift.

A last remark is in order. For reference, we can point out that by setting $\tan\alpha = 1$, we can define a 'deflection radius' ρ_D,

$$\rho_\mathrm{D} = \left(\frac{15\pi}{8} \frac{C_6}{m_\mathrm{H}\, v^2} \right)^{1/6}, \tag{C.5}$$

which is the radius below which the deflection of an incoming atom becomes significant; it is the analog of the well-known Weisskopf radius which describes the onset of a significant phase shift during a collision. For our experimental conditions, a numerical estimate shows that the deflection radius and the Weisskopf radius are of the same order-of-magnitude, implying some of the atoms otherwise affected by collisional are being kicked out of the beam. As explained in section 4, the estimates of the collisional frequency shifts obtained here, thus constitute upper limits for the effect in the Garching experiment [1].

ORCID iDs

U D Jentschura https://orcid.org/0000-0003-4967-5458

References

[1] Beyer A *et al* 2017 The Rydberg constant and proton size from atomic hydrogen *Science* **358** 79–85
[2] Fleurbaey H 2017 Frequency metrology of the $1S$–$3S$ transition of hydrogen: contribution to the proton charge radius puzzle *PhD Thesis* Université Pierre et Marie Curie, Paris VI https://hal.archives-ouvertes.fr/tel-01633631
[3] Horbatsch M and Hessels E A 2010 Shifts from a distant neighboring resonance *Phys. Rev.* A **82** 052519
[4] Yost D C, Matveev A, Peters E, Maisenbacher L, Pohl R, Kolachevsky N, Khabarova K, Hänsch T W and Udem T 2016 Spectroscopy of the hydrogen 1S–3S transition with chirped laser pulses *Phys. Rev.* A **93** 042509
[5] Matveev A *et al* 2013 Precision measurement of the hydrogen 1S-2S frequency via a 920 km fiber link *Phys. Rev. Lett.* **110** 230801
[6] Mohr P J, Newell D B and Taylor B N 2016 CODATA recommended values of the fundamental physical constants: 2014 *Rev. Mod. Phys.* **88** 035009
[7] Pohl R *et al* 2010 The size of the proton *Nature* **466** 213–6

[8] Pohl R *et al* 2016 Laser spectroscopy of muonic deuterium *Science* **353** 669–73
[9] Michelson A A 1895 On the broadening of spectral lines *Astrophys. J.* **2** 251–63
[10] Lorentz H A 1906 The absorption and emission lines of gaseous bodies *Proc. Acad. Sci. Amsterdam* **8** 591–611
[11] Sobel'man I I, Vainshtein L A and Yukov E A 1981 *Excitation of Atoms and Broadening of Spectral Lines* (New York: Springer)
[12] Adhikari C M, Debierre V, Matveev A, Kolachevsky N and Jentschura U D 2017 Long-range interactions of hydrogen atoms in excited states: I. 2*S*–1*S* interactions and Dirac-δ perturbations *Phys. Rev.* A **95** 022703
[13] Jentschura U D, Debierre V, Adhikari C M, Matveev A and Kolachevsky N 2017 Long-range interactions of excited hydrogen atoms: II. Hyperfine-resolved 2*S*–2*S* system *Phys. Rev.* A **95** 022704
[14] Jentschura U D, Adhikari C M, Dawes R, Matveev A and Kolachevsky N 2019 Pressure shifts in high–precision hydrogen spectroscopy: I. Long–range atom–atom and atom-molecule interactions *J. Phys. B: At. Mol. Opt.* **52** 075005
[15] Sobel'man I I 1972 *Introduction to the Theory of Atomic Spectra* (Oxford: Pergamon)
[16] Bethe H A and Salpeter E E 1957 *Quantum Mechanics of One- and Two-Electron Atoms* (Berlin: Springer)
[17] Adhikari C M, Debierre V and Jentschura U D 2017 Long-range interactions of hydrogen atoms in excited states: III. *nS*–1*S* interactions for $n \geqslant 3$ *Phys. Rev.* A **96** 032702
[18] Jentschura U D and Adhikari C M 2017 Long-range interactions for hydrogen: 6*P*–1*S* and 6*P*–2*S* systems *Atoms* **5** 48
[19] Chibisov M I 1972 Dispersion interaction of neutral atoms *Opt. Spectrosc.* **32** 1–3
[20] Ali A W and Griem H R 1965 Theory of resonance broadening of spectral lines by atom–atom impacts *Phys. Rev.* A **140** A1044–9
Ali A W and Griem H R 1966 *Phys. Rev.* A **144** 366
[21] Beyer A, Maisenbacher L, Khabarova K, Matveev A, Pohl R, Udem T, Hänsch T W and Kolachevsky N 2015 Precision spectroscopy of 2S–*n*P transitions in atomic hydrogen for a new determination of the Rydberg constant and the proton charge radius *Phys. Scr.* **T165** 014030
[22] Sutton A 1962 Measurement of the dissociation rates of hydrogen and deuterium *J. Chem. Phys.* **36** 2923–31
[23] Haas M *et al* 2006 Two-photon excitation dynamics in bound two-body Coulomb systems including AC Stark shift and ionization *Phys. Rev.* A **73** 052501
[24] Haas M 2006 *PhD Thesis* Ruperto-Carola University of Heidelberg, Heidelberg (unpublished)